Analysis of a centrifugal pump impeller using ANSYS-CFX

S.Rajendran[1] and Dr.K.Purushothaman[2]

[1]*Research Scholar, Department of Mechanical Engineering, Anna university of Technology, Chennai 600025, Tamilnadu, INDIA.*
[2]*Professor & Head, Department of Mechanical Engineering, St.Peter's College of Engineering and Technology, Avadi, Chennai, Tamilnadu, INDIA.*

Abstract

ANSYS software package was used to develop a three dimensional, fully turbulent model of the compressible flow across a complex geometry of impeller, such as those found in centrifugal pump. It is a most common pump used in industries and domestic applications. The Flow through centrifugal pump impeller is three dimensional and fully turbulence model. The present paper describes the simulation of the flow in the impeller of a centrifugal pump. The analysis of centrifugal pump impeller design is carried out using ANSYS-CFX. The complex internal flows in Centrifugal pump impellers can be well predicted through ANSYS-CFX. The numerical solution of the discredited three-dimensional, incompressible Navier-Stokes equations over an unstructured grid is accomplished with an ANSYS-CFX. The flow pattern, pressure distribution in the blade passage, blade loading and pressure plots are discussed in this paper.

Keywords- Centrifugal pump causing, Centrifugal pump impeller, Ansys-CFX, Efficiency. and Pressure

1. Introduction

A centrifugal pump is a kinetic device. Liquid entering the pump receives kinetic energy from the rotating impeller. The centrifugal action of the impeller accelerates the liquid to a high velocity, transferring mechanical (rotational) energy to the liquid. That kinetic energy is available to the fluid to accomplish work. In most cases, the work consists of the liquid moving at some velocity through a system by overcoming resistance to flow due to friction from pipes, and physical restrictions from valves, heat exchangers and other in-line devices, as well as elevation changes between the liquid's starting location and final destination. When velocity is reduced due to resistance encountered in the system, pressure increases. As resistance is encountered, the liquid expends some its energy in the form of heat, noise, and vibration in overcoming that resistance. The result is that the available energy in the liquid decreases as the distance from the pump increases. The actual energy available for work at any point in a system is a combination of the available velocity and pressure energy at that point.

Khin Cho Thin et. al. [1] have carried out computational analysis of a centrifugal pump and predicted performance for off-design volume flow rate and calculated impeller volute disc friction loss, slip, shock losses, recirculation losses and other friction losses. E.C. Bcharoudis et. al. [2] have contributed to reveal the flow mechanisms inside centrifugal impellers and studied performance by varying outlet blade angle. They observed a gain in head more than 7 % with increase in outlet blade angle from 20^{o} to 45^{o}. Motohiko Nohmi et. al. [3] have developed two types of cavitation CFD codes for centrifugal pump. They observed that at the cavitation, there is a breakdown of flow rate as throat is choked by cavities on both suction surface and pressure surfaces. Vasilios A. et. al. [4] studied computational analysis of centrifugal pump impeller by optimizing blade inlet geometry. John S. Anagnostopoulos [5] solved RANS equations for the impeller of centrifugal pump and developed fully automated algorithm for impeller design. M.H.Shojaee Fard and F.A.Boyaghchi [6] have carried out computational analysis on a centrifugal pump handling viscous fluids. They observed performance improvements in centrifugal pump with increase in the outlet blade angle due to decrease of wake formation at the exit of the impeller.

2. Pump specifications

The systematic research on the influence of the various design aspects of a centrifugal pump in its performance at various flow rates requires numerical predictions and experiments. The specifications of centrifugal

pump undertaken in the current analysis are shown in Table No.1.

Blade width b	20 mm
Inlet diameter D_1	150 mm
Outlet diameter D2	280 mm
Pump head H	10
Outlet blade angle β_2	20˚
Speed of the impeller N	925 rpm
Flow rate, Q	0.0125 m^3/sec
Specific speed $N_s = N\sqrt{Q}/H^4$	18.39
The diameter of impeller eye Do= K_0 $\sqrt[3]{(Q/N)}$ Where K_0 is the constant 4.5	43.5mm
Hydraulic Efficiency	83%
Number of Blades	6

Table No.1. Specifications of centrifugal pump

3. Meshing

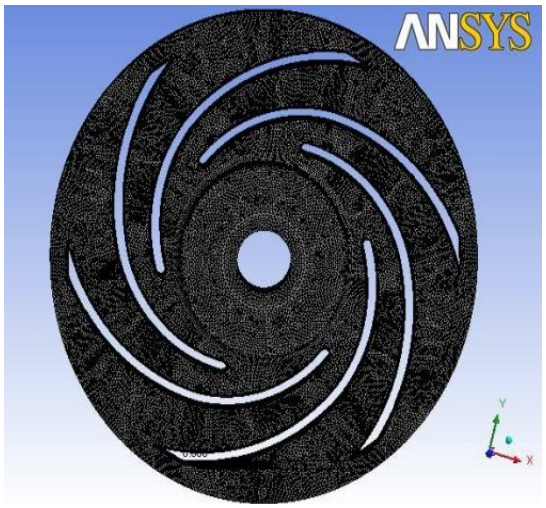

Fig.2 Unstructured mesh of the impeller

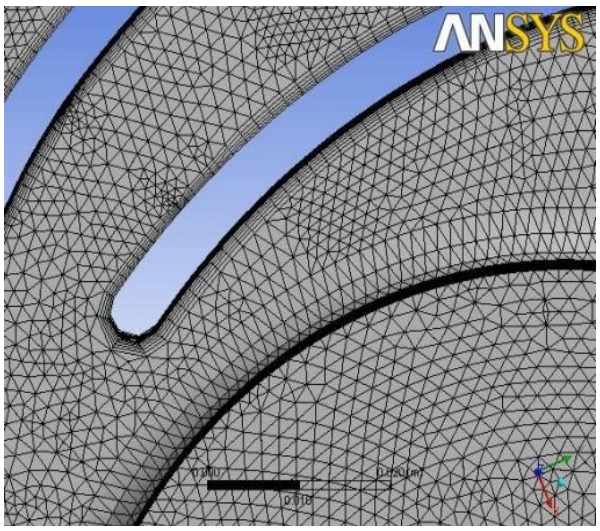

Fig.3 Mesh refinement around the blade surface and inflated layers

The geometry and the mesh of a six bladed pump impeller domain is generated using Ansys Workbench. An unstructured mesh with tetrahedral cells is also used for the zones of impeller and volute as shown in Fig.2.

The mesh is refined in the near tongue region of the volute as well as in the regions close to the leading and trailing edge of the blades. Around the blades, structured hexahedral cells are generated to obtain better boundary layer details. Fig.3 shows the mesh near the tongue region. A total of 3570268 elements are generated for the impeller domain. Mesh statistics are presented in Table 2.

1	Number of nodes	805234
2	Number of tetrahedral	3415244
3	Number of prisms	250987
4	Number of elements	3572269
5	Number of pyramids	910

Table 2. Mesh statistics are presented.

4. Boundary conditions

Centrifugal pump impeller domain is considered as rotating frame of reference with a rotational speed of 925 rpm. The working fluid through the pump is water at 25° C. k-ε turbulence model with turbulence

intensity of 5% is considered. Inlet static pressure and outlet mass flow rate of 12.5kg/s are given as boundary conditions. Three dimensional incompressible N-S equations are solved with Ansys-CFX Solver.

5. Results

Centrifugal pump impeller without volute casing is solved at designed mass flow rate of 12.5 kg/m^3. The performance results are presented in Table No.3. The head obtained by the CFD analysis is 9.4528 m/WG and total efficiency obtained is 91.1029%.

Sl.No	Descriptions	parameters
1.	Diameter of causing	0.280 m
2.	Rotational speed	942 rpm
3.	Volume of flow rate	0.0125 m^3/s
4.	Head (in)	9.25 m
5.	Head (out)	9.45 m
6.	Flow Coefficient	0.0931
7.	Head Coefficient	0.134
8.	Shaft power	14209.01 w
9.	Power Coefficient	0.0145
10.	Static Efficiency %	64.56
11.	Total Efficiency %	95.05

Table No.3: Centrifugal Pump Performance Results

5.1 Pressure Contours on a plane

Besides the centrifugal pump performance results, the local characteristics of the internal flow field is accomplished. The Pressure contours at different span wise locations of 10, 25, 50, 75, 90 and 100% are shown in Fig.4.

The pressure contours show a continuous pressure rise from leading edge to trailing edge of the impeller due to the dynamic head developed by the rotating pump impeller. It is observed that total pressure on pressure side of the blade is more than that of suction side. The difference of pressure from the pressure side to the suction side of the impeller blade is increasing from leading edge to trailing edge of the blade. The minimum value of the static pressure inside the impeller is located at the leading edge of the blades on the suction side

The total pressure patterns are varying along the span of the impeller. Low total pressures are observed near hub of the impeller. With increase in span, total pressures are increasing because of high dynamic head at tip of the blade. A low total pressure and high velocity is observed near the leading edge on suction side of the blade because of the vane thickness. At trailing edge of the blade total pressure loss is observed for all span wise locations due to the wake formation at trailing edge of the blade

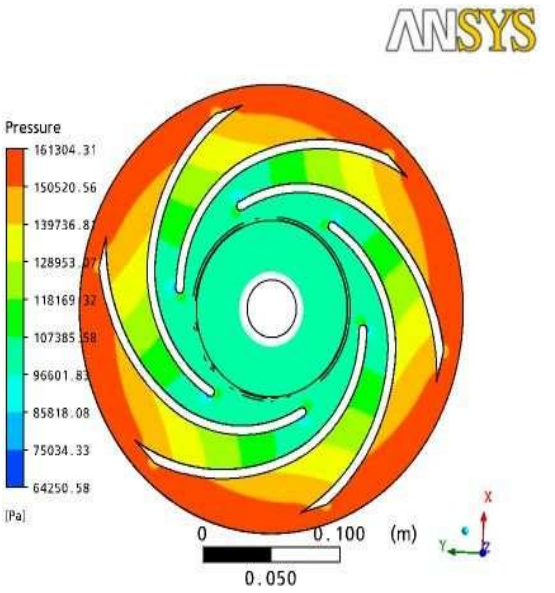

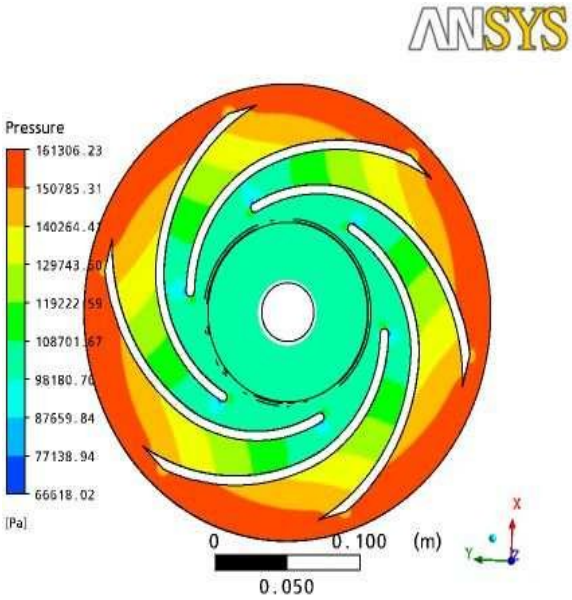

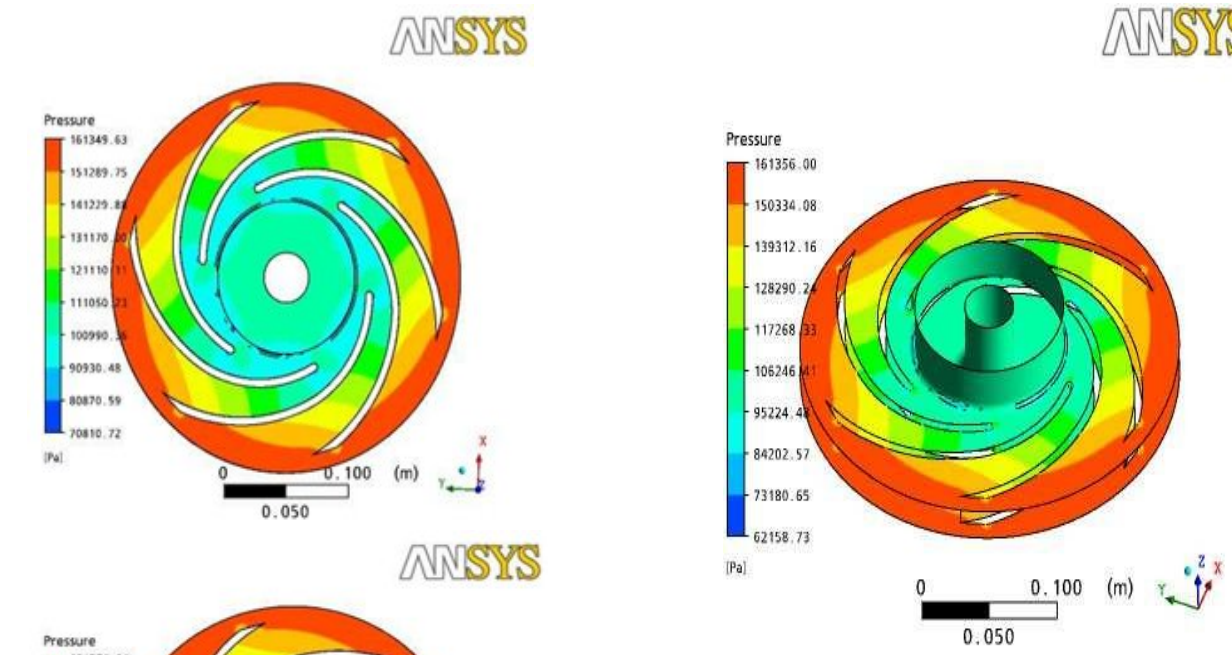

Fig.4 Pressure contours at different span wise locations of 10, 25, 50, 75, 90 and 100%

5.2 Circumferential Area Averaged Pressure

Circumferential area averaged pressure from hub to shroud variation with span is shown in Fig. 5. Till 50% span, increase in pressure is observed. After that uniform pressure is observed with span increments. A pressure difference of 2000Pa is observed between hub to shroud

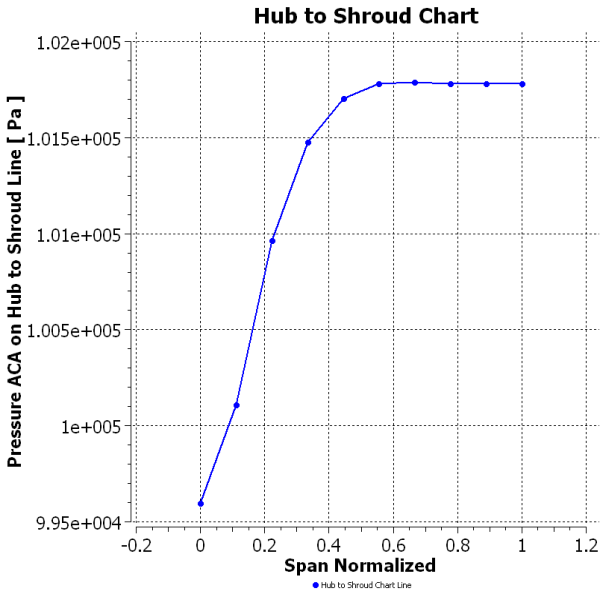

5.3 Blade loading at 50% span

Blade loading plot for the centrifugal impeller at

50% span is shown in Fig. 6. Gradual increase of pressure is observed with stream wise increment. High pressures on pressure side of the blade and low pressures on suction side of the blade are observed.

At leading edge, pressure drop on both pressure and suction side are observed due to the acceleration of the flow in to the impeller. At 10% stream wise location pressure drop is observed on pressure side of the blade. At trailing edge of the blade, pressure drop is observed due to the blade wake.

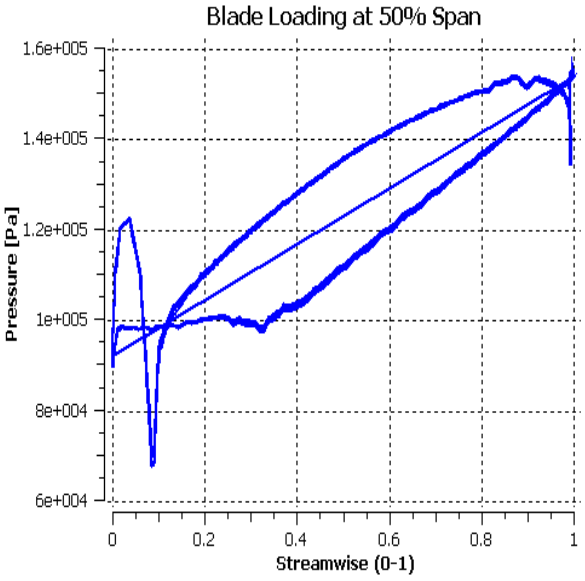

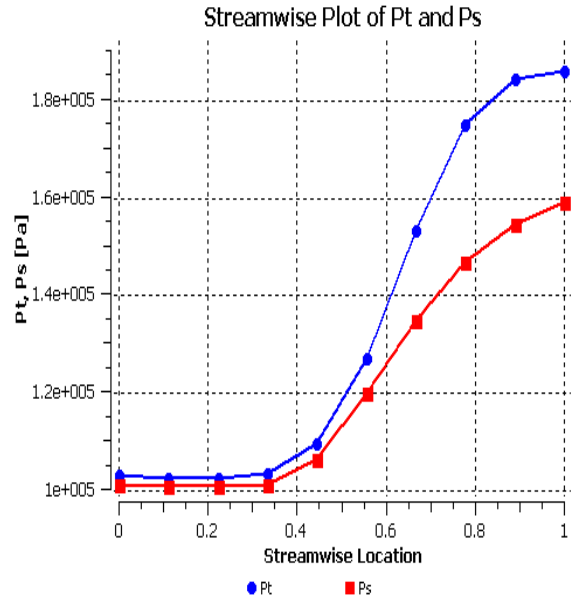

Fig.7. Stream wise variation of mass averaged total pressure and static pressure [Pa]

5.4 Stream wise variation of area averaged absolute velocity

Stream wise variation of area averaged absolute velocity is shown in Fig.8. From 30% stream wise location, the area averaged absolute velocity is increasing with stream wise increment due to the dynamic energy transfer from the impeller to the fluid. From 90% stream wise location, the area averaged absolute velocity is decreasing because of increase in pressure in outlet duct.

5.5 Stream wise variation of mass averaged total pressure and static pressure

Stream wise variation of mass averaged total pressure and static pressure is shown in Fig. 7. Gradual increase in total and static pressure from inlet to outlet is observed. At low stream wise locations the mass averaged total and static pressures are observed constant due to the inlet duct before the impeller.

From 30% stream wise location the pressures are increasing due to the dynamic energy transfer from the rotating impeller to the fluid. From 90% stream wise location the mass averaged total pressure is observed constant due to the absence of energy transfer in outlet duct. However, static pressure increment is observed because of diffusion in outlet duct.

5.6 Variation of mass averaged total pressure at blade leading edge and trailing edge

Variation of mass averaged total pressure contours at blade leading edge is shown in fig. 9. Mass averaged total pressure contours at leading edge show a drastic change in pressures near the blade leading edge. Variation of mass averaged total pressure contours at blade trailing edge is shown in Fig. 10. High mass averaged total pressures on pressure side of the blade and low mass averaged total pressures on suction side of the blade are observed. Near the trailing edge of the blade total pressure loss because of wake is observed.

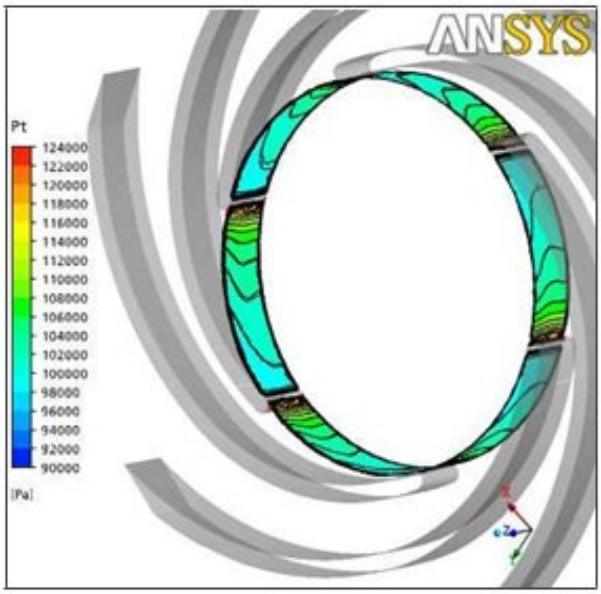

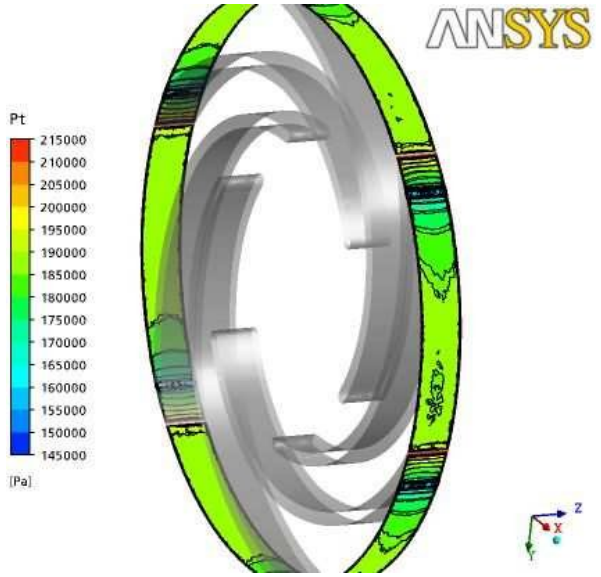

6. Conclusions

A centrifugal pump impeller is modeled and solved using computational fluid dynamics, the flow patterns through the pump, performance results, circumferential area averaged pressure from hub to shroud line, blade loading plot at 50 % span, stream wise variation of mass averaged total pressure and static pressure, stream wise variation of area averaged absolute velocity and variation of mass averaged total pressure contours at blade leading edge and trailing edge for designed flow rate are presented.

The CFD predicted value of the head at the design flow rate is approximately H=9.4528 m. The pressure contours show a continuous pressure rise from leading edge to trailing edge of the impeller due to the dynamic head developed by the rotating pump impeller. Near leading edge of the blade low pressure and high velocities are observed due to the thickness of the blade. Near trailing edge of the blade total pressure loss is observed due to the presence of trailing edge wake.

7. References

[1] Khin Cho Thin, Mya Mya Khaing, and Khin Maung Aye, "Design and Performance Analysis of Centrifugal Pump", World Academy of Science, Engineering and Technology pp46,2008.

[2] E.C. Bcharoudis, A.E. ilios ,M.D. Mentzos and D.P. Margaris, "Parametric Study of a Centrifugal Pump Impeller by Varying the Outlet Blade Angle", The open Mechanical Engineering Journal, pp75-83, 2008,.

[3] Motohiko Nohmi, Akira Goto, "Cavitation CFD in a Centrifugal pump", Fifth international symposium on cavitations, Osaka, Japan, november2003.

[4] Vasilios A. Grapsas, John S. Anagnostopoulos and Dimitrios E. Papantonis, "Hydrodynamic Design of Radial Flow Pump Impeller by Surface Parameterization", International Conference on Experiments / Process / System Modeling / Simulation / Optimization, Athens, 6-9 July, 2005.

[5] M.H.Shojaee Fard and F.A.Boyaghchi, "Studies on the influence of various blade outlet angles in a centrifugal pump when handling viscous fluids", American Journal of Applied Sciences pp.718-724, 2007.

[6] John S. Anagnostopoulos, "CFD Analysis and Design Effects in a Radial Pump Impeller", Wseas Transactions on Fluid Mechanics, Vol 1, July2006.